

Systematic study of interface trap and barrier inhomogeneities using I-V-T characteristics of Au/ZnO nanorods Schottky diode

I. Hussain, M. Y. Soomro, N. Bano, O. Nur, and M. Willander

Department of Science and Technology, Campus Norrköping, Linköping University, SE-60174 Norrköping, Sweden

(Received 14 March 2013; accepted 29 May 2013; published online 19 June 2013)

This paper presents in-depth analysis of I-V-T characteristics of Au/ZnO nanorods Schottky diodes. The temperature dependence I-V parameters such as the ideality factor and the barrier heights have been explained on the basis of inhomogeneity. Detailed and systematic analysis was performed to extract information about the interface trap states. The ideality factor decreases, while the barrier height increases with increase of temperature. These observations have been ascribed to barrier inhomogeneities at the Au/ZnO nanorods interface. The inhomogeneities can be described by the Gaussian distribution of barrier heights. The effect of tunneling, Fermi level pinning, and image force lowering has contribution in the barrier height lowering. The recombination-tunneling mechanism is used to explain the conduction process in Au/ZnO nanorods Schottky diodes. The ionization of interface states has been considered for explaining the inhomogeneities.

© 2013 AIP Publishing LLC. [<http://dx.doi.org/10.1063/1.4810924>]

I. INTRODUCTION

ZnO nanostructures possess a promising future owing to the variety of optical and electrical properties which are technologically useful for many nano scale devices. In recent years, ZnO nanostructures have been the subject of renewed interest with the aim of fabricating devices such as light emitting diodes (LEDs), laser diodes, UV detectors, and solar cells.¹ The production of high quality ZnO nanostructures based homo-junctions has proved elusive because of the difficulties in the growth of p-ZnO material.² Conversely, the fabrication of hetero-junctions and Schottky contacts on n-ZnO nanostructures allows the realization of electronics devices. Although considerable progress has been made in the fabrication of ZnO nanostructure-based Schottky diodes, many questions remain about the nature of the electrical transport and the interface states at the metal-ZnO interface.³ A stable and good quality rectifying metal contact on the n-ZnO surface is crucial for many optoelectronic applications and remains a challenge despite numerous recent investigations.³⁻⁶

The realization of high quality Schottky contacts on ZnO nanostructures seems to be difficult because of the interface states, the surface morphology, hydroxide surface contamination, and the subsurface defects, which all play important roles in the electrical properties of these contacts.⁷ In recent years, a number of process methodologies have been developed for the fabrication of reproducible high quality Schottky contacts on ZnO nanostructures, but controversies remain with regard to the Schottky barrier height and the factor of the ZnO Schottky contacts.^{7,8} The deviations in the barrier heights and the ideality factor have been proposed as having been caused by the effects of asymmetric contacts, and the influence of the interfacial layers and/or surface states.⁸

The interface of metal/ZnO nanorods play very important roles in many high-performance devices in optoelectronic, high temperature, high-frequency, and power

applications. Schottky diodes are of the simplest devices due to their technological importance. So the understanding of Schottky-barrier formation at these interfaces on a fundamental basis is therefore of great interest. Schottky diodes play an important role in devices operating at cryogenic temperatures as detectors, sensors, microwave diodes, gates of transistors, and infrared and nuclear particle detectors.⁹⁻¹¹ Therefore, analysis of the current voltage (I-V) characteristics of the Schottky diodes at room temperature does not give detailed information about their conduction process, the nature of barrier formation at the interface and interface states.¹²⁻¹⁷ The temperature dependence of the I-V characteristics allows us to understand different aspects of conduction mechanisms and the calculation of interface states.⁹⁻¹⁵

In low dimensional systems, the Schottky barrier height depends not only on the work functions of the metal but also on the pinning of the Fermi level by surface states, image force lowering, field penetration and the existence of an interfacial insulating layer, these effects change the absolute current value at very low bias via lowering the Schottky barrier. The deviation in barrier heights and the ideality factor and has simply been proposed by the impacts of asymmetric contact, the influence of interfacial layers and/or surface states.^{18,19} In fact, the surface of nanostructures should mostly be dominated by surface states because there are usually abundant surface states existing on the surface of these nanostructures.²⁰ However to the best of our knowledge, there have only few reports on Schottky contacts on ZnO nanostructures, but no report has been found to elucidate in depth analysis of I-V-T characteristics of ZnO nanorods Schottky diodes and how the surface states influence the barrier potential of the ZnO nanorods Schottky diodes. Therefore, the main aim of the present work is to investigate the barrier inhomogeneities at the ZnO nanorods Schottky barrier interface and systematic analysis was performed to extract information about the interface trap states by

temperature dependent current-voltage (I-V-T) measurements. The values of the ideality factor, the barrier height, and the density of interface states and were calculated.

II. EXPERIMENTAL DETAILS

To grow the ZnO NRs on Ag coated Si substrates, we used a low temperature chemical growth method. In this method, to improve the ZnO NR growth quality, distribution and density, a seed layer is spin-coated and baked for 30 min at 250 °C.²¹ Then, zinc nitrate hexahydrate ($\text{Zn}(\text{NO}_3)_2 \cdot 6\text{H}_2\text{O}$) was mixed with hexamethylene tetramine (HMT) ($\text{C}_6\text{H}_{12}\text{N}_4$) in equal molar concentrations, and the substrates were placed in the resulting solution for 4 h at 90 °C. We covered a small portion of the substrate before the growth of the ZnO NRs and Al was used for the back ohmic contact to ZnO nanorods. After growth, the samples were used to fabricate Schottky diodes. Prior to fabrication of the Schottky contacts, an insulating PMMA layer was deposited between the ZnO NRs. To ensure that no PMMA was on top of the ZnO NRs, oxygen plasma cleaning was performed prior to Au Schottky contact deposition. The Au metal contacts were formed on a group of ZnO NRs by thermal evaporation at a pressure of 2×10^{-7} Torr, and the contacts were formed as circular dots of 1 mm in diameter and 150 nm in thickness. The device structure was characterized by scanning electron microscopy (SEM), along with temperature dependent I-V measurements.

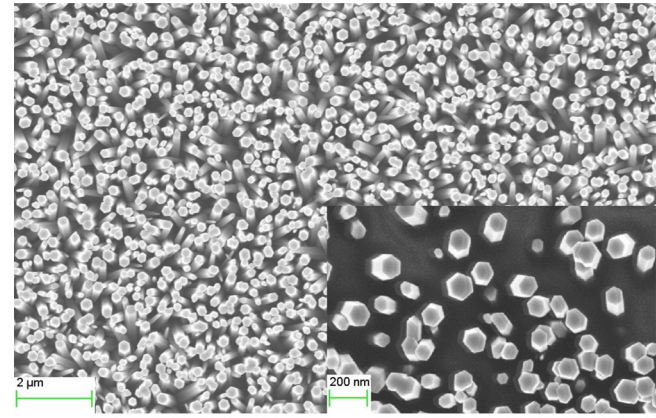
III. RESULTS DISCUSSION

The ZnO NRs grown were found to be aligned vertically and distributed uniformly as shown in the SEM image in Fig. 1(a). The inset shows the SEM image after spin coating insulating layer and followed by soft backing. The schematic diagram of the Au/ZnO nanorods Schottky diodes is shown in Fig. 1(b). The temperature dependent I-V characteristics of Au/ZnO NRs Schottky diodes in the temperature range of 100–420 K are shown in Fig. 2. The I-V characteristics show a kink structure which may be due to the tunneling current at low biases, and for large biases, it is dominated by the series resistance. Many models have been proposed to explain the excess leakage currents, including the thin barrier model²² and the field-emission/trap-assisted tunneling model.²³ Generally, total current consists of both thermionic emission and tunneling component. Assuming that the thermionic emission is the most predominant mechanism, the general form of the temperature dependence of current may be expressed as

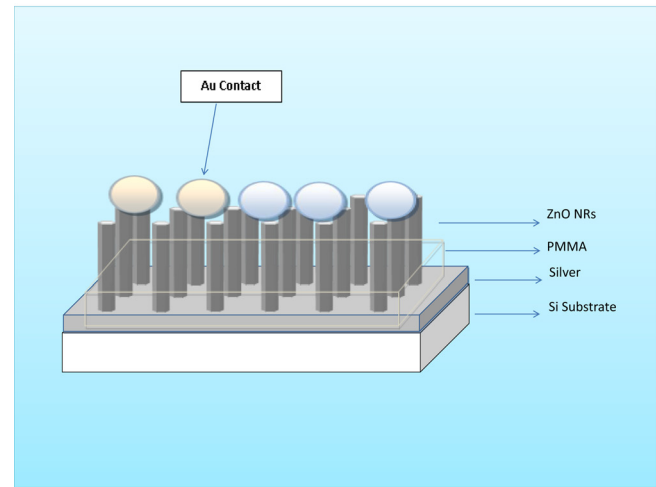
$$I = I_s \left[\exp\left(\frac{qV}{nkT}\right) - 1 \right], \quad (1)$$

where n and I_s are ideality factor and saturation current, respectively.

The values for the ideality factor n were obtained from the slope of the linear region of $\ln I$ vs V curves at each temperature using Eq. (1). At each temperature, saturation current I_s was obtained by extrapolating the linear region of $\ln I$ vs V curve to zero applied voltage and the barrier height ϕ_{B0} values were calculated from the following equation:



(a)



(b)

FIG. 1. (a) SEM image of as grown ZnO NRs and inset shows the SEM image after spin coating insulating layer and followed by soft backing. (b) Schematic illustration of Au/ZnO NRs Schottky diode.

$$I_s = AA^* \exp\left(-\frac{q\phi_{B0}}{kT}\right), \quad (2)$$

where A is diode area, A^* is the effective Richardson constant, and ϕ_{B0} is the barrier height.

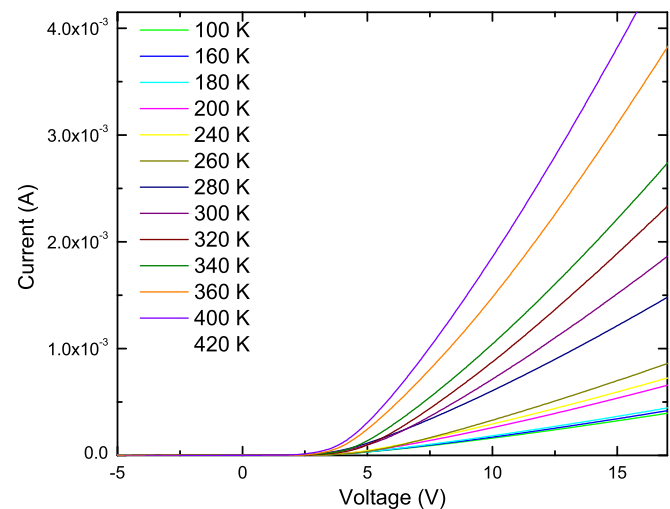


FIG. 2. I-V characteristics measured at different temperature for Schottky diode.

For an ideal diode, the diode ideality factor (n) should be nearly equal to unity. But in a real situation, it may increase due to the effects of series resistance and leakage current. In nanostructures based Schottky diodes, the tunneling current is not negligible and dominating mechanism under reverse bias. Also there are inherent difficulties when the base material would offer a considerable series resistance, which would cause a voltage drop across the junction. The current flows according to thermionic emission model only when the ideality factor (n) is near unity but with an increase in n , the barrier height would deviate from the true value. For the ZnO NRs, the surface states and the effective carrier concentration have important influence to the contact barrier. A slight inhomogeneity of the surface states and carrier concentration at the two ends of the ZnO nanorods can result in different Schottky barriers. In such a case, generalized Norde method could be used to evaluate the effective barrier height, series resistance, and diode ideality factor (n) from I–V measurement.¹² The values of effective barrier potential and diode ideality factor measured at different

temperatures for Au/n-ZnO Schottky diode are shown graphically in Figs. 3(a) and 3(b), respectively.

Figure 3(a) shows that the ideality factor decreased with increasing temperature which explains the current transport across the metal semiconductor interface is temperature dependent. Thus, the electrons at low temperature would be able to cross only the lower barriers and therefore current transport will be dominated by current passing through the lower Schottky barrier only contributing to a large ideality factor. With increasing temperature, the electrons would acquire significant energy to cross higher barrier. As a result, the effective barrier height will increase with the temperature and bias voltage culminating in lower ideality factor at higher temperature. This increment can be explained by taking into account of the interface state density distribution, quantum mechanical tunneling, and image force lowering across the barrier of Schottky diodes.

The barrier height could be seen to increase with temperature as shown in Fig. 5(b). The increase in barrier heights with the increase in temperature from 100 K to 400 K may be associated with the increase in available charge carriers to be transported across the barrier for Fermi level equalization. The value of barrier height for ZnO nanorods based Schottky contact is lower than the thin-film based ZnO Schottky diodes. Lower values of barrier heights ascribed to an enhanced electric field at the depletion region due to the nano-Schottky junction. The strong local electric fields are induced at the sharp edge morphologies of nano-Schottky junction which increases in magnitude by the enhancement factor (γ_a). In the nano-junction surfaces, localized free electron oscillations are produced at the surface and the lightning rod effect contributing to the enhancement of electric field.²⁴

The ideality factor was found to increase, while ϕ_{B0} decreases with decreasing temperature ($n = 9.8$ and $\phi_{B0} = 0.78$ eV at 100 K, and $n = 1.6$ and $\phi_{B0} = 1.2$ eV at 400 K). The values of the ideality factor obtained indicate that the current transport mechanism consists of both the trap-assisted tunneling and the thermionic emission. It is

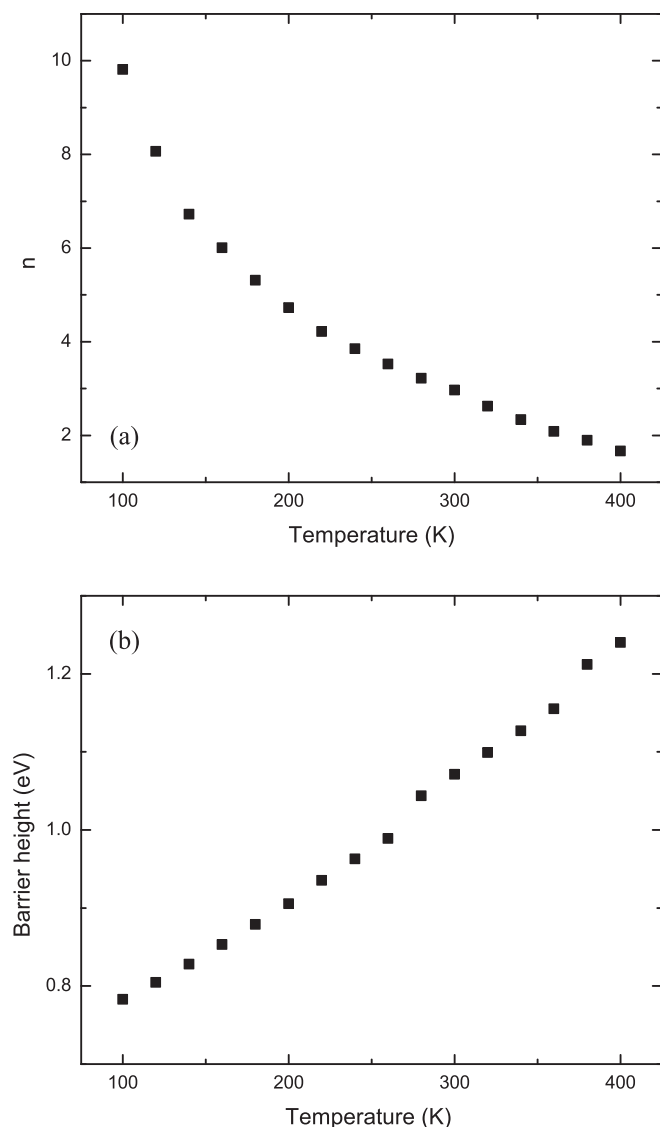


FIG. 3. (a) Temperature dependence of ideality factor for Schottky diode. (b) Temperature dependence of barrier height for Schottky diode.

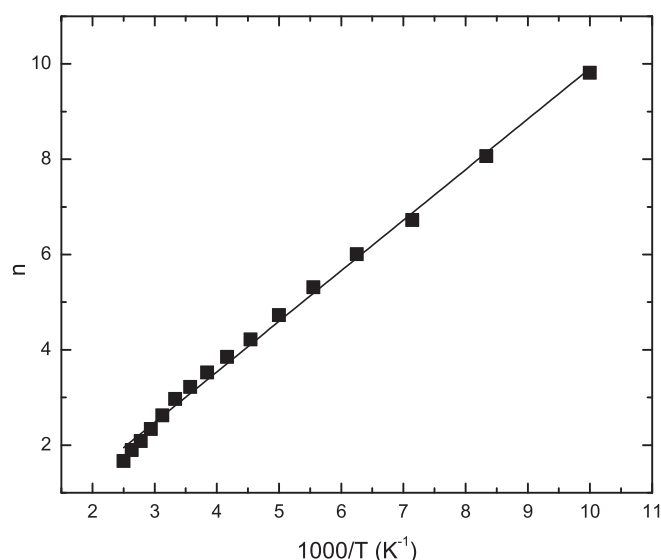


FIG. 4. Plot of n vs. $10^3/T$ for Schottky diode.

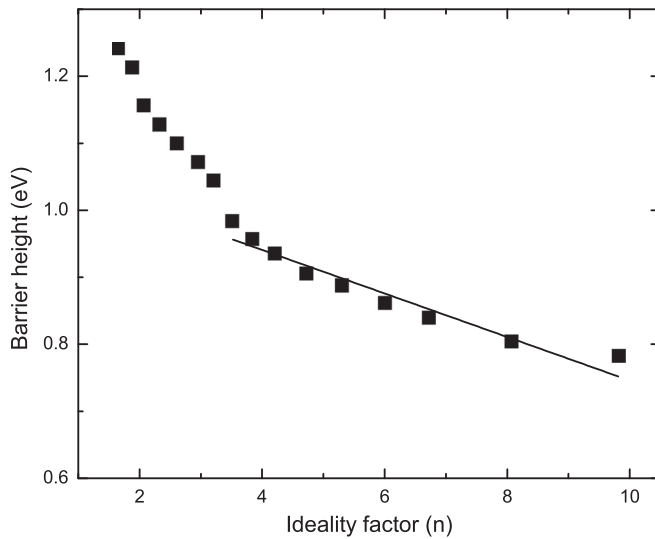


FIG. 5. Variation of barrier height with ideality factor.

worth nothing that the product of n and temperature seems to remain constant in the investigated temperature range. On the basis of information available in the literature,²⁵ the constant product means that the diode carrier transport should be dominated by trap-assisted tunneling at temperatures well below 300 K. Above 300 K, the thermionic emission of carriers at the Schottky barrier should dominate the diode carrier transport and causes the diode ideality factor to approach unity. When a metal is evaporated on the semiconductor surface the metal and semiconductor do not make intimate contact because of interfacial layer. The high values of the ideality factor at low temperatures are probably due to the potential drop in the interfacial layer.²⁶

For the investigation of the temperature dependence of barrier height and ideality factor, we use Richardson plot of saturation current. Equation (2) can be written as

$$\ln\left(\frac{I_s}{T^2}\right) = \ln(AA^*) - \frac{q\phi_{B0}}{kT}. \quad (3)$$

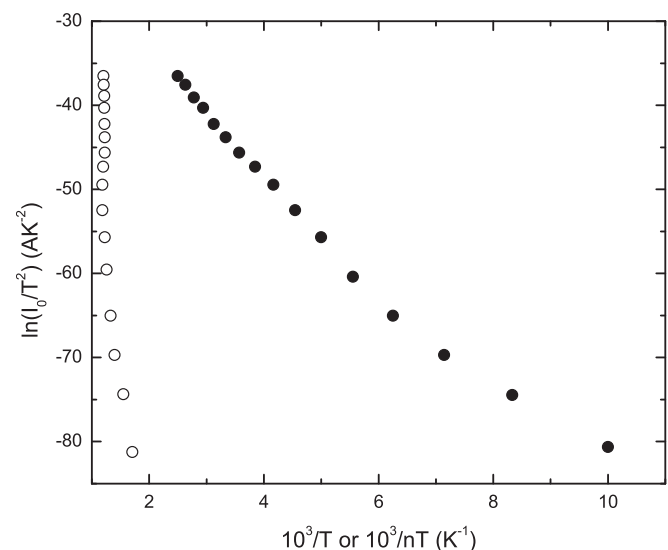
Fig. 4 shows a plot of n vs. $10^3/T$ reporting the temperature dependence of ideality factor n . The temperature dependence of the barrier height is shown in Fig. 4. This temperature effect (of the barrier height and ideality factor in Schottky diodes) is called the T_0 effect.^{27,28} The T_0 effect can be connected either with the lateral inhomogeneity of the barrier height or with the role of the recombination, interface state density distribution,^{29,30} image force lowering,³¹ and tunneling current components.^{27,28,32} Some authors have mentioned that the ideality factor, barrier height, saturation current and all functions derived from them can be explained and connected with the lateral distribution of barrier height due to local enhancement of electric field which can also yield a local reduction of the barrier height.^{28,33} Özdemir *et al.* explained that the Gaussian distribution of the barrier height in-homogeneity is caused by the local change of electric field.⁹

There is linear correlation between experimental value of barrier height and n as calculated experimentally. This

linear dependence of barrier height and n for higher ideality factors theoretically and experimentally has been reported by different authors.^{12–14} Figure 5 shows a linear relationship between the barrier height and n only for higher ideality factor, which has been explained by lateral inhomogeneities of the barrier heights in the Schottky diode. Tung *et al.* have reported the existence of inhomogeneity at barrier interface by considering the variation barrier height with ideality factor.¹⁵ Thus, it can be said that the increase of the ideality factor and decrease of the barrier height especially at low temperature are probably caused by the barrier height inhomogeneities. Figure 5 is the signatures for the presence of lateral inhomogeneities in the Au/ZnO nanorods interface.

Moreover for the further evaluation of the barrier height, one may also make use of the Richardson plot of saturation current. Figure 6 (indicated by filled circles) shows a conventional activation energy $\ln(I_s/T^2)$ vs. $10^3/T$ plot (Richardson plot). Experimentally investigations results in a $\ln(I_s/T^2)$ vs. $10^3/T$ plot significantly differing from linearity. However, at low temperatures, the dependence of $\ln(I_s/T^2)$ vs. $10^3/nT$ gives a straight line (Fig. 6). The non-linearity of the conventional $\ln(I_s/T^2)$ vs. $10^3/T$ is caused by the temperature dependence of the barrier height and ideality factor. Analysis of the I-V characteristics based on thermionic emission theory usually reveals an abnormal decrease in the barrier height and an increase in the ideality factor n with a decrease in temperature. The decrease in the barrier height at low temperatures leads to nonlinearity in the activation energy $\ln(I_s/T^2)$ vs. $10^3/T$ plot.

In fact interface states are always introduced due to oxidation of semiconductor surfaces from extended air exposure, surface dipoles, incomplete covalent bonds, hydrogen and chemical reactions during fabrication processes and sharp discontinuity between semiconductor crystal and metal.^{34–36} The chemical reactions at the metal-ZnO interface play an important role in Schottky barrier formation. These chemical reactions will result in an increase in the density of oxygen vacancies (V_O) close to the interface. The creation of oxygen

FIG. 6. Richardson plots of $\ln(I_s/T^2)$ vs. $10^3/T$ and $10^3/nT$ for Schottky diode.

vacancies becomes energetically more favorable near a metal-ZnO interface. This is too deep to contribute significantly to the unintentional n-type conductivity of ZnO but is shallow enough to cause Fermi level pinning at the ZnO interface. It has been proposed that oxygen vacancies strongly influence the Schottky barrier formation by pinning the ZnO Fermi level close to the V_O defect level at ~ 0.7 eV below the conduction band minimum. However, good quality Schottky contacts to ZnO have not been observed to degrade in performance with time, so the V_O creation probably occurs immediately with the contact formation. Therefore, the V_O is the dominant reason for the inhomogeneity and the ZnO nanorods have more surface states because of their large surface area and small diameter.⁷ The solution chemistry used to grow the ZnO NRs provide some insight into the nature of this surface variation and these surface states also may be controlled by solution chemistry.

Such defects produce a large density of interface states which are continuously distributed in the energy within the forbidden gap and cause leakage currents to flow. Taking into account the series resistance and voltage dependent ideality factor, the density of interface states (N_{SS}) is extracted using I-V characteristics³⁷

$$N_{SS} = \frac{1}{q} \left[\frac{\varepsilon_i}{\delta} \{n(V) - 1\} - \frac{\varepsilon_S}{W_D} \right]. \quad (4)$$

Here, W_D is the width of the space charge region extracted from experimental C - V data.

Bias dependant effective barrier height (ϕ_e) and the energy of interface states with respect to the conduction band edge ($E_C - E_{SS}$) are obtained by using following equations:

$$\phi_e = \phi_{bo} + \left(1 - \frac{1}{n(V)}\right)(V - IR_S), \quad (5)$$

$$E_C - E_{SS} = q(\phi_e - V). \quad (6)$$

The density of interface states as a function of interface state energy ($E_C - E_{SS}$) for Au Schottky diode is shown in Fig. 7.

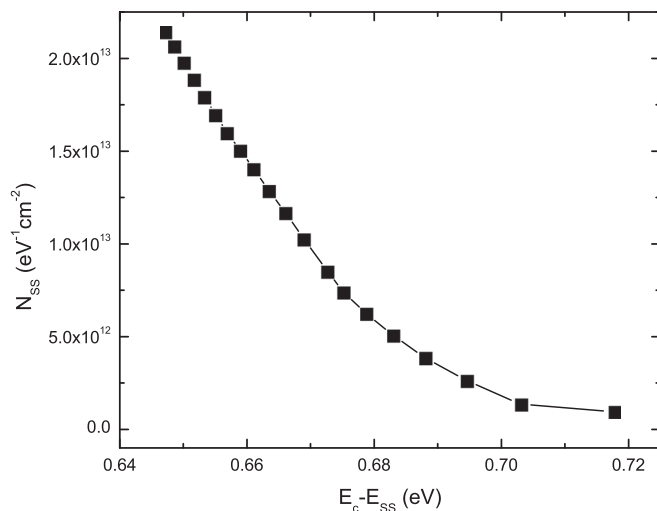


FIG. 7. Interface state density distribution profiles as a function of $E_C - E_{SS}$.

The values of the density of interface states were determined to be $2 \times 10^{13} \text{ cm}^{-2} \text{ eV}^{-1}$. The exponential rise in the interface state density towards the bottom of the conduction band is very apparent; the ionization of interface state by hot electron reduced the band bending as well as the Schottky barrier height. As the Schottky barrier height changes, a characteristic asymmetric conductance change is expected. The value of density of surface state ($2 \times 10^{13} \text{ cm}^{-2} \text{ eV}^{-1}$) is not very high. These surface states are formed in ZnO nanorods because of their large surface area and small diameter.³⁸ When electrons are excited to conduction band, they are trapped by these states and hence the electrical behavior of diode is affected. The effects of interface states are more important for compound semiconductor nano structure as their surfaces have more defects.³⁹

IV. CONCLUSIONS

In conclusion, it can be speculated from the diode parameters obtained by I-V-T method that the spatial inhomogeneities of the barrier heights is an important factor and could not be ignored in the electrical characterization of the Schottky diodes. Therefore, the detailed I-V-T characteristics of the Schottky diodes have been investigated at different temperatures. The barrier height value and ideality factor at different temperature for Schottky diodes were obtained from I-V-T measurements, the decrease in the barrier height and an increase in the ideality factor have been observed with temperature. The large value of ideality factor and barrier inhomogeneities demonstrates other mechanism like recombination and tunneling which are involved in explaining the electrical transport properties of Au/ZnO nanorods Schottky diodes. The effect of tunneling, Fermi level pinning and image force lowering have contribution in the barrier height lowering. The recombination—tunneling mechanism is used to explain the conduction process in Au/ZnO nanorods Schottky diodes. The ionization of interface states has been considered for explaining the inhomogeneities. The results yield that the interface states play a very important role in the current flow mechanism and these states must be kept as low as possible in order to reduce the surface recombination and tunneling.

¹M. Willander, O. Nur, Q. X. Zhao, L. L. Yang, M. Lorenz, B. Q. Cao, J. Zúñiga Pérez, C. Czekalla, G. Zimmermann, M. Grundmann, A. Bakin, A. Behrends, M. Al-Suleiman, A. El-Shaer, A. CheMofor, B. Postels, A. Waag, N. Boukos, A. Travlos, H. S. Kwack, J. Guinard, and D. Le Si Dang, *Nanotechnology* **20**, 332001 (2009).

²M. W. Allen, S. M. Durbin, and J. B. Metson, *Appl. Phys. Lett.* **91**(5), 053512 (2007).

³H. L. Mosbacker, Y. M. Strzhemechny, and B. D. White, *Appl. Phys. Lett.* **87**(1), 012102 (2005).

⁴S. J. Pearton, D. P. Norton, K. Ip, Y. W. Heo, and T. Steiner, *Prog. Mater. Sci.* **50**, 293 (2005).

⁵A. Salomon, D. Berkovich, and D. Cahen, *Appl. Phys. Lett.* **82**, 1051 (2003).

⁶S.-H. Kim, H.-K. Kim, and T.-Y. Seong, *Appl. Phys. Lett.* **86**, 112101 (2005).

⁷I. Hussain, M. Y. Soomro, N. Bano, O. Nur, and M. Willander, *J. Appl. Phys.* **112**, 064506 (2012).

⁸X. Zhang, F. Hai, T. Zhang, C. Jia, Xianwen Sun, L. Ding, and W. Zhang, *Microelectron. Eng.* **93**, 5 (2012).

- ⁹A. F. Özdemir, A. Türit, and A. Kökçe, *Semicond. Sci. Technol.* **21**, 298 (2006).
- ¹⁰S. Chand and J. Kumar, *Semicond. Sci. Technol.* **10**, 1680 (1995).
- ¹¹Ş. Karataş, Ş. Altındal, A. Türit, and A. Özmen, *Appl. Surf. Sci.* **217**, 250 (2003).
- ¹²M. Sharma and S. K. Tripathi, *J. Appl. Phys.* **112**, 024521 (2012).
- ¹³T. Tunç, I. Dökme, S. Altındal, and I. Uslu, *Optoelectron. Adv. Mater. Rapid Commun.* **4**(7), 947 (2010).
- ¹⁴S. Sankar Naik and V. Rajagopal Reddy, *Adv. Mater. Lett.* **3**(3), 188 (2012).
- ¹⁵R. T. Tungs, *Mater. Sci. Eng. R* **35**, 1 (2001).
- ¹⁶G. M. Vanalme, L. Goubert, R. L. Van Meirhaeghe, F. Cardon, and P. vanDaele, *Semicond. Sci. Technol.* **14**, 871 (1999).
- ¹⁷Zs. J. Horváth, *Solid-State Electron.* **39**, 176 (1996).
- ¹⁸W. I. Park, G. C. Yi, J. W. Kim, and S. M. Park, *Appl. Phys. Lett.* **82**, 4358 (2003).
- ¹⁹Z. Y. Zhang, C. H. Jin, X. L. Liang, Q. Chen, and L. M. Peng, *Appl. Phys. Lett.* **88**, 073102 (2006).
- ²⁰M. Haase, H. Weller, and A. Henglein, *J. Phys. Chem.* **92**, 482 (1988).
- ²¹M. Vafaei and H. Youzbashizade, *Mater. Sci. Forum* **553**, 252 (2007).
- ²²T. Hashizume, J. Kotani, and H. Hasegawa, *Appl. Phys. Lett.* **84**, 4884 (2004).
- ²³E. J. Miller, E. T. Yu, P. Waltereit, and J. S. Speck, *Appl. Phys. Lett.* **84**, 535 (2004).
- ²⁴J. Yu, M. Shafiei, W. Wlodarski, Y. X. Li, and K. Kalantar-zadeh, *J. Phys. D: Appl. Phys.* **43**, 025103 (2010).
- ²⁵T. Nagatomo, M. Ando, and O. Omoto, *Jpn. J. Appl. Phys., Part 1* **18**, 1103 (1979).
- ²⁶D. T. Quan and H. Hbib, *Solid-State Electron* **36**, 339 (1993).
- ²⁷F. Roccaforte, F. La Via, V. Raineri, R. Pierobon, and E. Zanoni, *J. Appl. Phys.* **93**, 9137 (2003).
- ²⁸E. Ayyildiz, H. Cetin, and Zs. J. Horvath, *Appl. Surf. Sci.* **252**, 1153 (2005).
- ²⁹R. T. Tung, *Phys. Rev. B* **45**, 13509 (1992).
- ³⁰C. R. Crowell, *Solid-State Electron* **20**, 171 (1977).
- ³¹E. H. Rhoderick and R. H. Williams, *Metal-Semiconductor Contacts* (Clarendon, Oxford, 1988).
- ³²M. W. Allen and S. M. Durbin, *Appl. Phys. Lett.* **92**, 122110 (2008).
- ³³Zs. J. Horvath, V. Rakovics, B. Szentpali, S. Püppi, and K. Zdansky, *Vacuum* **71**, 113 (2003).
- ³⁴B. G. Streetman and S. K. Banerjee, *Solid State Electronic Devices*, 6th ed. (Prentice-Hall, Englewood Cliffs, NJ, 2006).
- ³⁵L. J. Brillson *J. Phys. Chem. Solids* **44**, 703 (1983).
- ³⁶F. Léonard and A. A. Talin, *Nature Nanotechnol.* **6**, 773 (2011).
- ³⁷H. C. Card and E. H. Rhoderick, *J. Phys. D: Appl. Phys.* **04**, 1589 (1971).
- ³⁸X. Liu, X. Wu, H. Cao, and R. P. H. Chang, *J. Appl. Phys.* **95**, 3141 (2004).
- ³⁹M. Sochackia, J. Szmidt, M. Bakowskib, and A. Werbowya, *Diamond Relat. Mater.* **11**, 1263 (2002).